Substituent effects on the equilibria between cyclopropylcarbinyl, bicyclobutonium, homoallyl, and cyclobutyl cations

Sean P. Larmore and Pier Alexandre Champagne*

Department of Chemistry and Environmental Science, New Jersey Institute of Technology, Newark NJ 07102, USA

ABSTRACT: The cyclopropylcarbinyl (CPC) and bicyclobutonium (BCB) structures of the $C_4H_7^+$ cation have been proposed as intermediates in various synthetic transformations forming cyclopropylcarbinyl, cyclobutyl, or homoallyl products. It has recently been recognized that such cations, when generated from chiral electrophiles, are themselves chiral and can react with nucleophiles stereospecifically. However, the CPC and BCB cations are in equilibrium with each other and with other related structures such as the cyclobutyl (CB) and homoallyl (HA) cations, from which stereospecificity is not guaranteed. Currently, the effect of substitution on the composition of cation mixtures containing CPC/BCB/CB/HA cations is not understood, precluding the prediction and control of the major products generated from such cations. Using Density Functional Theory and DLPNO-CCSD(T) calculations, we have studied the electronic and steric effects on the equilibria between mono- and polysubstituted $C_4H_7^+$ cations. Our results indicate that electron-donating groups at the C1 position favor CPC structures, while BCB/CB structures are favored for the C2 position and HA structures for the C3/C4 positions. Electron-withdrawing groups yield shallower potential energy surfaces where many related structures are energetically accessible. Strong Hammett correlations (σ^+) are observed for the various substituent effects, which appear to be additive in nature. In addition, BCB cations with more substituents are energetically destabilized compared to CPC cations, except with donating substituents at the C2 position. This work provides a predictive model for the major structures observed in mixtures of CPC/BCB/CB/HA cations, for given substituent patterns.

Cyclopropylcarbinyl and bicyclobutonium cations ($C_4H_7^+$) have been of great scientific interest since Roberts' 1951 report that cyclobutyl and cyclopropylcarbinyl electrophiles solvolyze quickly to the same mixture of cyclobutyl, cyclopropylcarbinyl, and homoallyl products, hinting at a common, stabilized intermediate.[1] After many years of scientific debate, the $C_4H_7^+$ intermediates are now understood as a mixture of triply degenerate σπ-bisected cyclopropylcarbinyl (CPC) **I** and non-classical bicyclobutonium (BCB) **II** cations (Figure 1A),[2-4] the latter being the more stable structure (by 1.8 kcal/mol from MP2 calculations).[5-7] Solvolysis experiments of substituted cyclobutyl or cyclopropylcarbinyl electrophiles provided complex product mixtures in which the major component seems unpredictable, even for simple substitution patterns (Figure 1B).[8-20] Nevertheless, over the years multiple synthetic approaches have reported CPC/BCB and cyclobutyl (CB) cations as intermediates toward cyclopropylcarbinyl,[21-25] cyclobutyl,[26, 27] and homoallyl (HA) products.[22, 28, 29] Such cations have also been proposed as intermediates in the biosynthesis of various terpenes, using DFT calculations as support.[30-43]

An exciting property of CPC/BCB cations that has been rediscovered recently is that they can be intermediates in stereospecific transformations as their bridged nature ensures that they react with nucleophiles faster than they rearrange. For instance, Feringa, Houk and Fujita reported in 2018 that cycloheptenyl bromide **III** undergoes an enantiospecific rearrangement to its cyclohexenyl derivative **IV** under Lewis acid catalysis, a process that involves CPC cation **V**.[44] Similarly, Marek has published a series of reports starting in 2020, discussing how cyclopropylcarbinols **VI** form homoallylic products **VII** with high diastereoselectivity, as long as no aromatic substituent is located at the R^3 or R^4 positions.[45-50] Our group studied this system computationally and showed that CPC intermediate **VIII** is responsible for the observed selectivity.[51] This cation only rearranges faster than nucleophilic trapping when R^3 is an aryl substituent, which enables a classical homoallylic cation to intervene, leading to reduced specificity. Recently, Anderson and Duarte reported on the acid-mediated rearrangement of bicyclobutane amides **IX**, forming cyclopropylcarbinyl or cyclobutane products **X** or **XI**, both in good diastereoselectivity, depending on slight changes in substitution on the cation **XII**.[52] The electrophilic opening of strained bicyclobutanes, which generate BCB/CPC/CB cations,[53, 54] have recently garnered a lot of attention for the formation of cyclobutanes and cyclobutenes.[55-58]

Overall, reactions involving CPC/BCB cations have demonstrated a great potential for the stereospecific

synthesis of highly-substituted CPC, CB or HA products, yet it is difficult to predict the major isomers expected for a given substituent pattern, let alone influence the product mixture to favor a desired isomer. This is because such cations can rearrange between multiple structures that are in equilibrium when barriers to interconversion are significantly lower than barriers to nucleophilic attack. In order to better predict and control the outcomes of such reactions, a holistic understanding on the effects of substituents on the equilibria between CPC/BCB and related cations is warranted. We now report our Density Functional Theory (DFT) study of those effects, showing how different substituent groups at various positions on the core ($C_4H_7^+$) structure impact the delicate equilibria between these intermediates.

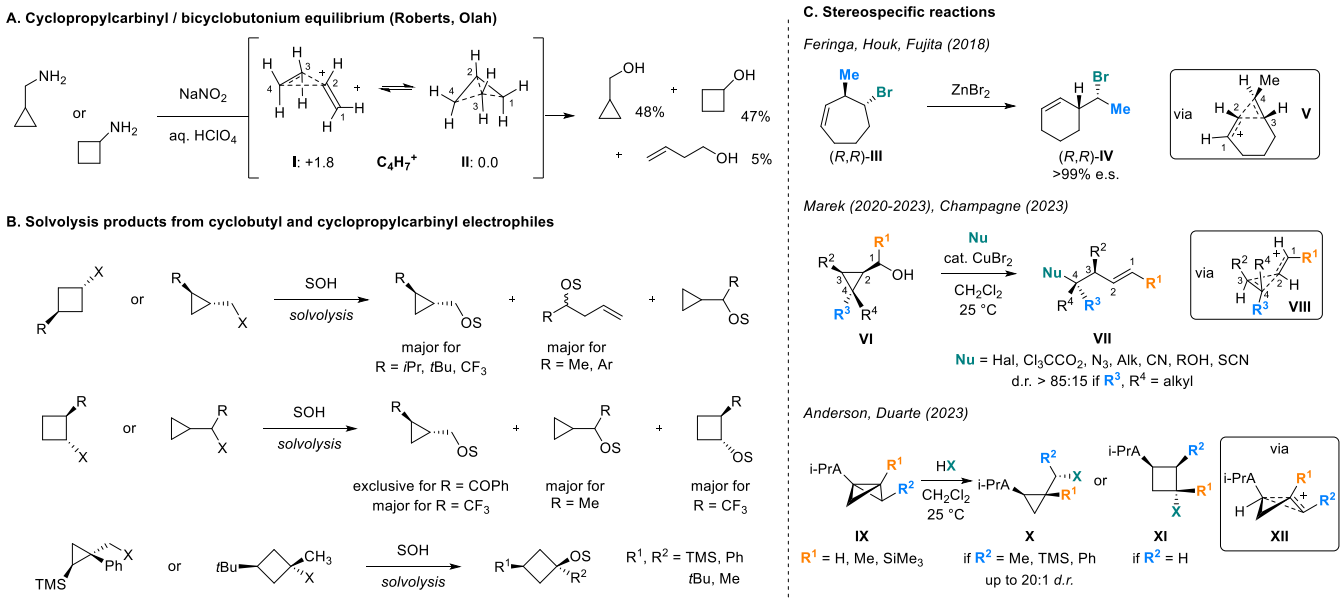

Figure 1. A) Experimental and computational results on the $C_4H_7^+$ system. Energies (in kcal/mol) are from ref. 7. B) Results from the solvolysis of some cyclopropylcarbinyl or cyclobutyl electrophiles. SOH: Alcoholic solvent or nucleophile. C) Recent uses of CPC/BCB cations in stereospecific transformations. i-PrA: isopropylamide

Computational methodology

DFT calculations were performed using Gaussian 16. For geometry optimizations, the ωB97X-D functional with the 6-31+G(d,p) basis set and the SMD solvation model for CH_2Cl_2 (a representative polar solvent) were used. Vibrational frequency analysis was used to confirm structures as either minima or transition structures (TSs) and to obtain thermodynamic corrections to enthalpy and free energy. Single-point energy (SPE) refinements were then obtained at the DLPNO-CCSD(T)/Def2-TZVPP level of theory. The free energies presented in the main text are obtained by adding the free energy corrections to the SPE. This combination of methods was shown to provide accurate results for the base $C_4H_7^+$ system as well as the complex Marek system in our previous work.[51] Full computational details can be found in the Supporting Information.

We first sampled the potential energy surface (PES) of the $C_4H_7^+$ system and located four main structures: cyclopropylcarbinyl (CPC), bicyclobutonium (BCB), homoallyl (HA), and cyclobutyl (CB) cations (Figure 2). Our methods, when implicit solvation is considered, find that the BCB structure is favored over the CPC by 1.5 kcal/mol, which is in line with *ab initio* calculations for this system (see Figure 1A). This is unique to the base system, as previous computational investigations of substituted $C_4H_7^+$ cations have shown BCB cations that are stable minima are rare.[7, 18-20, 31, 34, 35, 39, 59, 60] Interestingly, our calculations indicate that the CB cation is also a minimum in this system, despite it being 12.5 kcal/mol higher in free energy than the CPC. Lastly, we have identified the HA cation as a high-energy TS in the $C_4H_7^+$ system,[6] leading to the 1-methylallyl cation through a hydride shift (see Figure SI1-A).[13, 61, 62] Stable HA cations have, however, been located for hydroxy-substituted systems,[18] and in various biosynthetic pathways.[31, 33, 36, 38, 40] Solvation has no major impact on the geometry of the structures, but influences the BCB/CPC relative free energies.

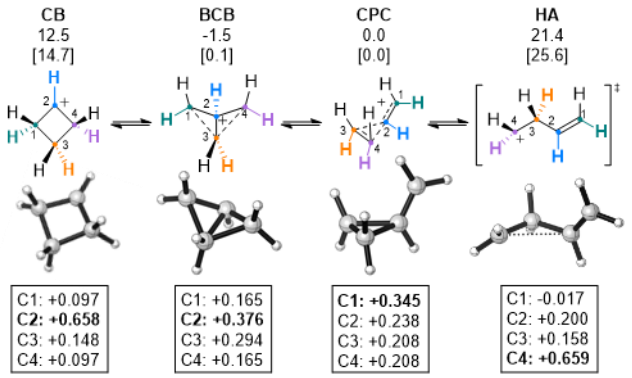

Figure 2. Structures, energies, and NBO charges for $C_4H_7^+$ cations. Plain text energies obtained in SMD (DCM) solvation, [bracketed] energies obtained for gas phase. Colored hydrogen atoms are in the *exo* positions on BCB and CPC cations.

Natural Bond Orbital (NBO) charge calculations on these structures highlight their differences in charge distribution. Unsurprisingly, both the CB and HA cations have the highest concentrations of charge on C2 and C4, respectively, which is in line with the trigonal planar, classical nature of the sp^2-hybridized electron-deficient carbon. On the other hand, the CPC and BCB cations display significant charge delocalization due to their bridged structures. In BCB, C2 and C3 bear significant charge, while for CPC the four carbons share the charge somewhat equally, with C1 having the largest electron deficiency. Based on the charge differences, we expected significant electronic effects and elected to first understand how they would impact the PES of these cations. To this end, we have selected 20 substituents of various donating or withdrawing electronic properties, from a Hammett σ^+ of 0.79 (NO_2) to −1.7 ($N(CH_3)_2$).[63] The complete list of considered substituents and their Hammett σ+ values can be found in Table SI2. We optimized BCB and CB cations with those substituents at positions C1, C2 and C3, and CPC and HA cations with substituents at positions C1, C2 and C4. Structures were generated by attaching substituent groups to the optimized $C_4H_7^+$ structure of interest, which was then followed by a minimum geometry optimization. In cases where optimization did not lead to the target structure, we performed TS optimizations instead. When those yielded the expected structure, both adjacent minima were checked to ensure that no ground state exists for that structure. In a few cases, neither minimum nor TS optimization yielded the desired geometry. In these rare cases we use the closest comparable stationary point on the PES to complete our analysis. The substituents induce major geometric deviations from the base $C_4H_7^+$ geometry, but all BCB, CB, CPC, and HA structures were obtained with this methodology. However, due to these deviations, it is important to properly define how we classify each structure in terms of geometric properties. These geometric definitions and their rationale can be found in the SI.

Results and discussion

Electronic effects

We first investigated the effect of substitution at the C2 position (Figure 3), focusing specifically on the equilibrium between CPC and BCB structures. For each substituent, the free energy difference between the BCB and corresponding CPC structure was plotted against the Hammett σ+ value, used to quantify the donating/withdrawing ability. There is a strong correlation between BCB stability and the strength of the electron-donating group (EDG) at C2, the strongest of which favor BCB-like structures by up to 54.1 kcal/mol. Conversely, strong electron-withdrawing groups (EWGs) favor CPC-like structures, although this effect is not as pronounced, with the strongest EWGs only favoring the CPC structure by at most 2.9 kcal/mol. This is strong evidence that C2 substitution is likely to favor BCB/CB structures in experimental systems.

We also note the key role that conjugation plays in stabilizing the BCB structure, which is especially relevant for π-donating (+R) groups. In fact, for all studied π-donating substituents (aromatics, OH, NH_2, etc.), the puckered BCB cations spontaneously optimize to planar cyclobutyl (CB) cations that maximize conjugation with the R group (see pink/purple points in Figure 3). Intrinsic Reaction Coordinate (IRC) analysis shows that during the rearrangement from CB to CPC, BCB-like structures are encountered (see Figure SI1-B) in steep sections of the IRC. Notably, even for the most electron-withdrawing aromatic C_6F_5 (σ^+ = 0.18), which could be expected to form the puckered BCB structure, CB cations are instead favored. This highlights the impact of aromatic groups at the C2 position in stabilizing CB versus BCB cations, though their Hammett values might indicate otherwise. This also demonstrates a potential limitation of Hammett σ^+ values in this study, as they measure the stabilization of a cationic center separated by a phenyl ring.

While all π-donating substituents spontaneously optimize to stable CB minima, all other substituents (i.e. non-π donating groups) also feature the CB structure as a minimum. The CB structure for these non-π donating groups are always higher in energy than the corresponding BCB by anywhere from 1.5 (R = Cl) to 15.8 (R = NO_2) kcal/mol (See Figure SI2 for all values). Thus, it is likely that interconversion between BCB stereoisomers through a CB cation is possible in cases where this barrier is low enough, as shown recently by Creary.[64] To our surprise, there are few substituents that allow both the CPC and BCB structures to be minima on the PES. These include H, SiR_3, Cl, and the strong EWGs CO_2CH_3, CF_3, CN, and NO_2 (blue points in Figure 3), and the free energy difference between the structures is at most ±10 kcal/mol. For other substituents, either the CPC is a TS (pink and green points) and/or the CB cation replaces the BCB (pink and purple points).

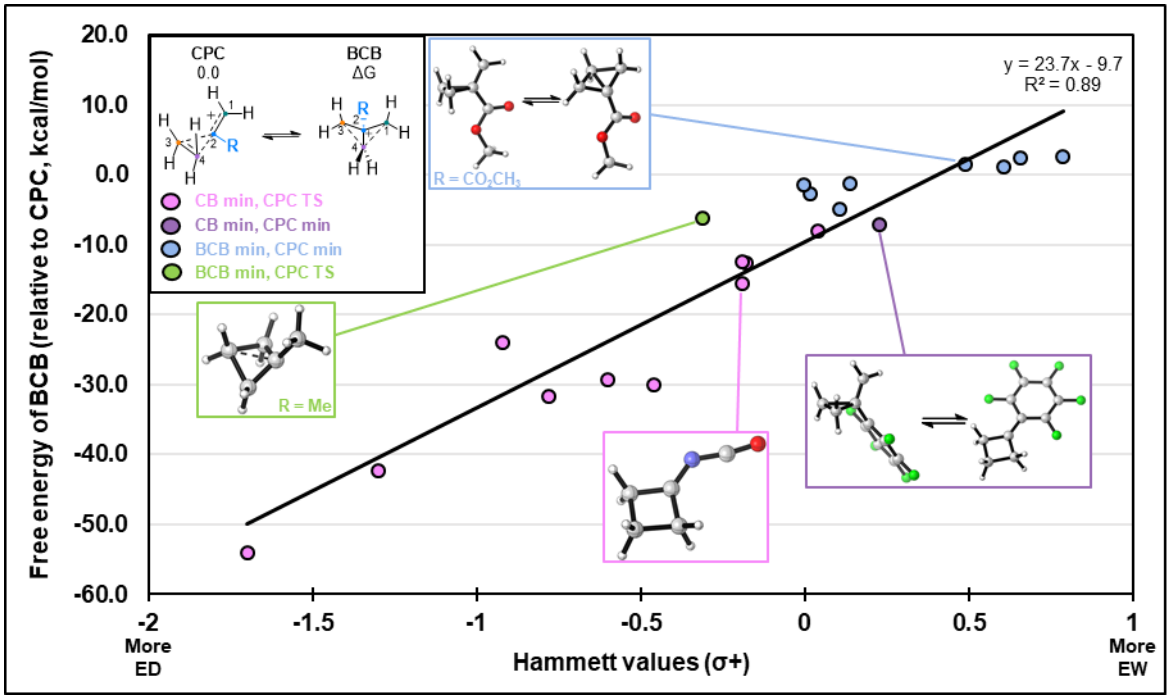

Figure 3. Effect of C2 substitution on the relative free energy (kcal/mol) between BCB and CPC cations.

Next, we wanted to consider the role that a substituent at C4 can play on the predominant structures of these cations. Based on our previous investigations on the Marek system,[51] we anticipated that substitution at C4 would play a key role in the equilibrium between CPC and HA structures. To investigate this hypothesis more rigorously, we plotted the energy difference between CPC and HA structures versus the Hammett constants for each substituent, finding a similar trend (Figure 4A). Specifically, our results show that EDGs at C4 greatly favor the HA structure over the CPC structure by up to 49.4 kcal/mol for the strongest EDGs. Moving from high ED to high EW ability, there is a steady increase in energy for the HA in comparison to the corresponding CPC cation, until the CPC becomes more stable relative to the HA, which becomes a TS (green and blue points) leading to the allylic system. For the strongest EWGs, the CPC can be favored by up to 26.9 kcal/mol. Since the HA structure predominantly places positive charge on C4 (Figure 2), EDGs on C4 greatly stabilize the HA structure, while EWGs decrease the stability of the structure in comparison to the CPC cation. Once again, π-donating (+R) groups' ability to stabilize adjacent carbocations seems somewhat underestimated by the Hammett σ^+ values. To our surprise, the vast majority (15/20) of substituents feature the HA structure as a minimum on their PES (purple and pink points, Figure 4A), often within ±20 kcal/mol from the CPC structure. This makes rearrangements through HA cations a possibility for many systems, emphasizing the role of this structure in the PES of CPC/BCB cations. Moreover, since the HA structures we have tested are only secondary cations, it is likely that the HA would be further promoted through additional substitution making it a tertiary carbocation.

Interestingly, for strong EDGs, whose HA cation is highly stabilized, the corresponding "CPC" structure is a TS on the PES (see pink points in Figure 4A). Geometrically, these TSs are not fully CPC cations, but display some BCB character, akin to a CPC-to-BCB TS in the $C_4H_7^+$ system (Figure SI-1D). We use these structures because no C4-substituted CPC cations exist as stationary points on the PES for these substituents. Instead, this "CPC" TS simplifies the PES and directly connects the C1-substituted CPC minimum to the C4-substituted HA minimum (see Figures SI-1C and SI7). On the opposite end of the spectrum, some strong EWGs also feature similar "CPC" structures as TSs on the PES (see blue points in Figure 4A). In such cases, this TS connects C1-BCB minima (Figure SI-1E), which are discussed in more detail below.

Upon seeing this strong trend between HA and CPC structures for C4 substitution, we wondered how the corresponding BCB structures might compare. From the CPC structure, there are two BCBs that are accessible, one which forms a bond between C1 and C4 placing the substituent at C3, while the other forms a bond between C1 and C3, placing the substituent at C1 (Figure 4B). Interestingly, we find no correlation between the Hammett constants and the free energy difference between CPC and either BCB structures (see Figure SI4). Independent of electron-donating or -withdrawing ability, these CPC and BCB structures are always close in energy (Figure SI7), with the CPC being favored by at most 11.7 kcal/mol (R=NCO) and the BCB being favored by at most by 4.6 kcal/mol

(R=CF_3). This indicates that, when CPC cations are minima and don't spontaneously open to HA cations, there are multiple rearrangements that are possible through BCB cations, leading to potential scrambling of the structures found in solution.

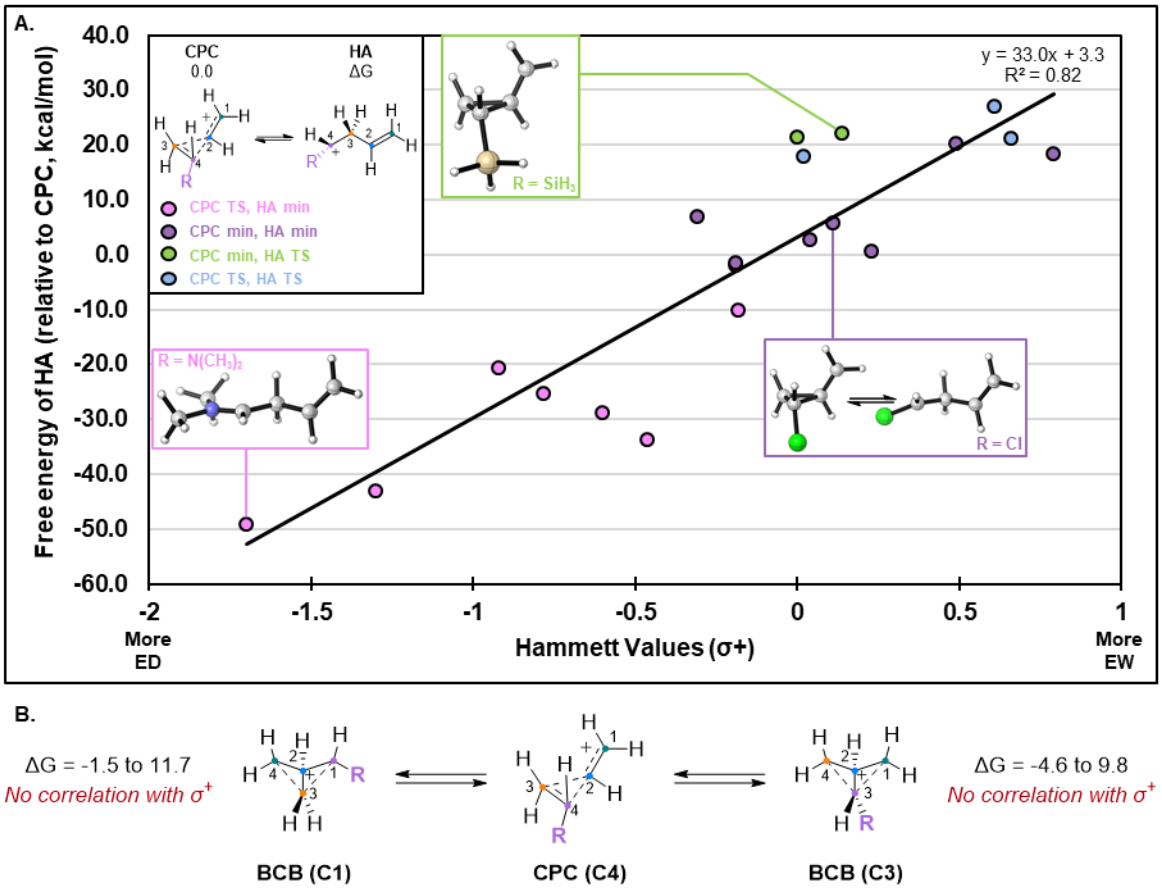

Figure 4. A) Effect of C4 substitution on the relative free energy (kcal/mol) between CPC and HA cations. B) Rearrangements from **CPC (C4)** for which no free energy correlation with Hammett constants is found. Minimum and maximum BCB free energies (kcal/mol) are relative to the CPC (C4) structure. Colored carbons are representative of the structural reorganization between structure, but carbon labels are consistent with our labeling convention from Figure 2.

Next, we investigated the effect of C1 substitution on CPC cations, by comparing the relative free energy of CPC structures to both BCB (Figure 5A) and HA (Figure 5B) structures as a function of substituents. Together, these data indicate that the C1 position has a great influence over the energy of the CPC cation, which was anticipated based on the large NBO charge on this carbon (Figure 2). First, the CPC-BCB graph (Figure 5A) shows that EDGs at the C1 position increase the energy gap between CPC and BCB structures, while EWGs narrow it. It is likely that EDGs strongly stabilize the CPC structure with its most positive carbon being C1, while having a much smaller impact on BCBs, leading to the observed trend. Conversely, EWGs favor the less positively-charged BCB-C1 position over the CPC (+0.165 vs. +0.345 NBO charge, respectively, Figure 2). Interestingly, only 7 substituents are predicted to lead to BCBs as minima (NO_2, CN, CF_3, $COOCH_3$, SiH_3, $SiMe_3$, and H, green points), all of which have Hammett σ^+ values larger than or equal to 0. All other substituent groups feature the "BCB" as a TS, though it is important to note that these TSs have significant CPC character and closely resemble the "CPC" TSs from Figure 4A (pink points). Indeed, these TSs also connect C1-substituted CPCs to C4-substituted CPCs or HAs (see Figures SI-1C and SI7). As discussed previously, we use these non-ideal structures since no other stationary points exist on the PES to characterize the BCB.

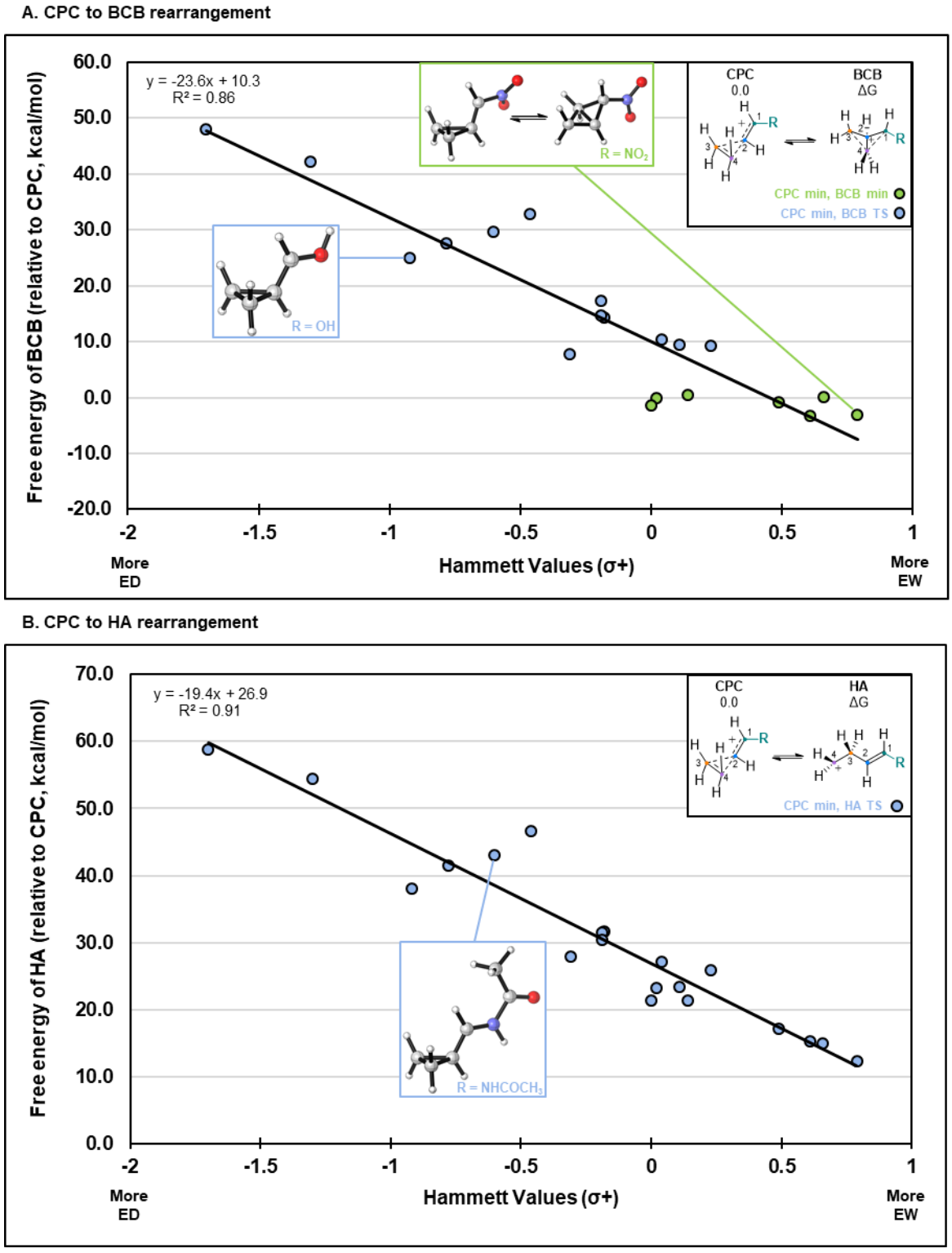

Figure 5. Effects of C1 substitution on the free energy (kcal/mol) difference between A) BCB vs CPC or B) HA vs CPC.

Comparisons between CPC and HA structures with substitution on C1 (Figure 5B) depict a similar picture of CPC stability. Once again, EDGs greatly increase the energy gap between CPC and HA structures, while EWGs decrease it. As reasoned previously, this indicates that EDGs on C1 greatly stabilize the CPC structure in relation to an HA intermediate, where the substituent at C1 bears little influence on the positive carbon C4. Notably, all computed HA structures are TSs as the primary HA cations are not minima and lead to the allylic cation directly. Interestingly, even with substitution present at the C4 position, substitution at C1 still has a significant stabilizing effect on

CPC vs HA structures. When a phenyl substituent is present at C1, the trend for HA vs. CPC (established in Figure 4) is skewed, favoring the CPC structure, and increasing the relative free energy of HA structures by approximately 13.8 kcal/mol (see Figure SI6). Notably, this energy value is in line with our prediction for the single-substitution stabilization of the CPC provided by a phenyl ring at the C1 position vs C4 position (14.3 kcal/mol, see Figure SI7, R=Ph, structures 2 and 5). Thus, it is plausible that effects of multiple groups add somewhat linearly (except in cases with steric interference) in polysubstituted systems. Overall, Figure 5 shows that as the ED ability of C1 substituents increases, the CPC cation becomes a deeper intermediate in comparison to both HA and BCB structures. Thus, this indicates that C1 substitution has major influence over the energy and stability of CPC-like cations.

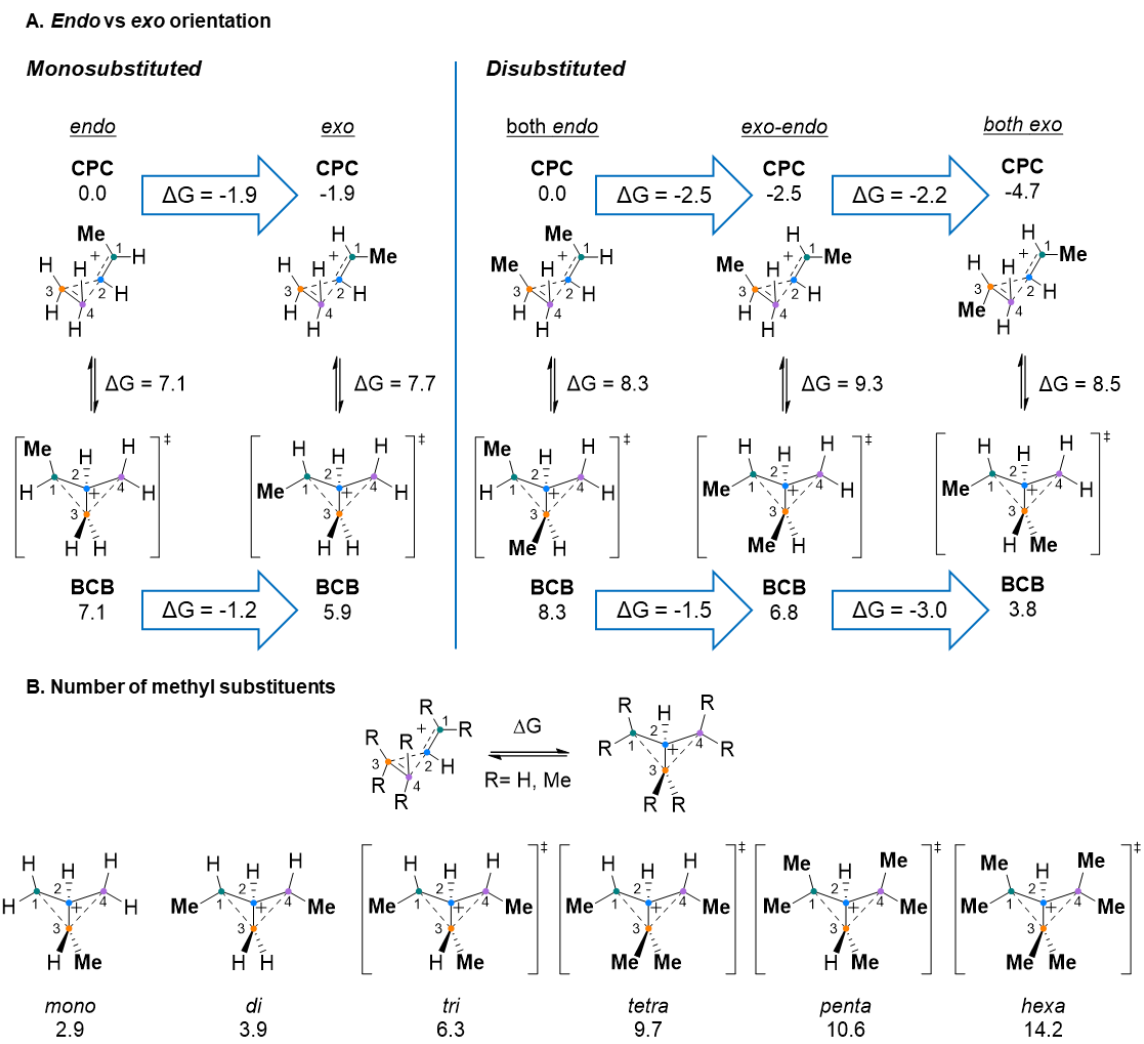

Figure 6. Steric effects on CPC and BCB cations. A) Exchange of methyl groups from *endo* to *exo* positions. Free energies (kcal/mol) are relative to the *endo* CPC structures. B) Relative free energy between symmetrical BCBs and their corresponding CPC structures with increasing number of methyl substituents. All free energies are in kcal/mol.

Steric effects

In addition to the electronic effects highlighted above, we wanted to gain additional insight into how steric forces might impact these various equilibria. We first explored how having substituents in the *endo* or *exo* positions of CPCs and BCBs affect their relative energy, computing structures with one or two methyl groups (Figure 6A). We find that, for structures bearing a set number of methyl groups, having them in the *exo* positions is consistently more favorable. For mono- and di-substituted CPC cations, each *endo*-to-*exo* replacement provides between 1.9 to 3.3 kcal/mol in stabilization (see Figure SI8 for all structures not shown in Figure 6A). A similar stabilization (1.2 to 3.0 kcal/mol) is obtained for BCB structures, so that overall, the relative free energy of BCB vs CPC structures is not heavily impacted by *endo* to *exo* substitution. In cases where isomerization of *endo* to *exo* structures is possible, usually enabled by an open HA cation, this energy difference might play in role in determining product stereochemistry.

In contrast to this, we find that the total number of substituents has an impact, as with increasing numbers of methyl substituents, the relative free energy of BCBs vs the

corresponding CPC structures increases (Figure 6B). In the unsubstituted case (Figure 2), the BCB is 1.5 kcal/mol more stable than the CPC. For a monomethyl cation, the BCB is 2.9 kcal/mol higher in free energy than the CPC, while in the hexamethyl case this difference is 14.2 kcal/mol. In addition to their higher relative energy, BCB cations with three or more methyl groups are TSs, while the CPC cations remain minima throughout. When a methyl is present at the tertiary C2 position, a similar trend exists but the relative energy between BCB and CPC structures is reduced by 7-10 kcal/mol (Figure SI9) and the BCB structures are minima on the PES. This is in line with the 6.0 kcal/mol BCB stabilization that a C2 methyl group affords (Figure 3). Overall, these trends indicate that the BCB is slightly more sterically strained compared to the CPC structure, and that BCBs that are minima are less likely for more substituted systems When compared to the electronic effects we uncovered for these systems, the steric effects are small, but may become a dominant factor when bulkier groups are present, favoring the CPC structure.

Conclusion

As carbocations are high-energy intermediates, their trapping by nucleophiles involve early, reactant-like TSs. Through the Hammond postulate, cationic intermediates that are more stable should thus get trapped with lower activation barriers. In the case of BCB/CPC cations, rearrangements often have larger activation energies than nucleophilic trapping, so the cation formed directly from the electrophile is likely to be captured preferentially. However, as these bridged cations have multiple electrophilic positions,[51] product mixtures are still expected to form when nucleophiles attack CPC/BCB cations, with stereoelectronic, dynamic, and/or counter-anion effects playing a role in determining the products formed and the stereoselectivity.

We have shown that electronic effects have major consequences for the preferred structures of CPC/BCB/HA equilibria, allowing us to propose a model for the prediction of preferred structures (Figure 7). For C2-substituted (tertiary) systems (Figure 7A), only one of each CPC, BCB and CB cation is available on the PES. For π-donating and aromatic substituents at C2, even electron-deficient ones, the only stable structure is the sp^2-hybridized, flat cyclobutyl cations **CB III**, from which unselective nucleophilic attack to cyclobutanes can be expected. Elimination to form cyclobutene products would also be available from **CB III**. For cations with non-aromatic EWGs at C2, or for EDGs that are not π-donating (e.g. alkyl groups), the **CPC I** and **BCB II** cations are similar in energy and in equilibrium, with the CPC being more favored for EWGs and the BCB for EDGs. As such, we reason that the C2-substituted systems with EDGs should lead to more cyclobutyl products, while those with EWGs should lead to more CPC or HA products.

In contrast to the relative simplicity of C2-substituted systems, CPCs/BCBs substituted at the secondary C1/C3/C4 positions have highly complex PESs due to the various structures in equilibrium (Figure 7B). In those scenarios, the nature of the electrophile should impact the content of the cationic mixture. For electrophiles with strong π-donating or electron rich aromatic groups that initially form **CPC IV**, rearrangement through **BCB V** is energetically inaccessible (requiring at least 14.3 kcal/mol) and CPC or HA products are expected. Similarly, if **CPC VI** is initially formed, the cations will spontaneously rearrange to the highly-stable **HA VII** and get trapped, forming HA products or butadienes upon elimination. Indeed, the tendency for EDGs to promote these deep minima is consistent with fewer reported cases of highly-alkylated BCB minima in comparison to reported CPC and HA structures. [7, 18-20, 31, 34, 35, 39, 59, 60]

For EWGs, neutral substituents, and electron-deficient aromatics (Ar), most of the PES is accessible as the minima are shallower, with several minima and TSs relatively close in energy. For instance, we predict that **CPC IV** is the lowest-energy structure for CN, C_6F_5, SiH_3, Cl, *p*-$NO_2C_6H_4$, *p*-ClC_6H_4, NCO, and Me, while **BCB V** is the most stable for NO_2, CF_3, CO_2CH_3, $SiMe_3$, and H. **CPC VI** is a stable minimum for most non-donating substituents, always within 10.0 kcal/mol of **BCB V** and **CPC IV**. For strong EWGs, SiR_3 and H, **HA VIII** is a TS to the allylic cation and thus high in energy compared to **CPC IV**. Overall, due to the shallowness of these PESs, we expect that the identity of the electrophile and dynamical effects will impact the final product distributions upon trapping of the cations, making these cases harder to predict.

Overall, our results provide insight into how the complex equilibrium at play between CPC, BCB, and HA cations is impacted by various substituent groups. We hope that our results can be a useful tool for experimentalists to gain additional mastery over these reactions as well as a starting point for future computational studies on these nuanced cations. Indeed, the additivity of these electronic effects for multiply-substituted systems, in addition to their interplay with steric effects which might become relevant for such systems, remains to be quantified. This work will be reported in due course.

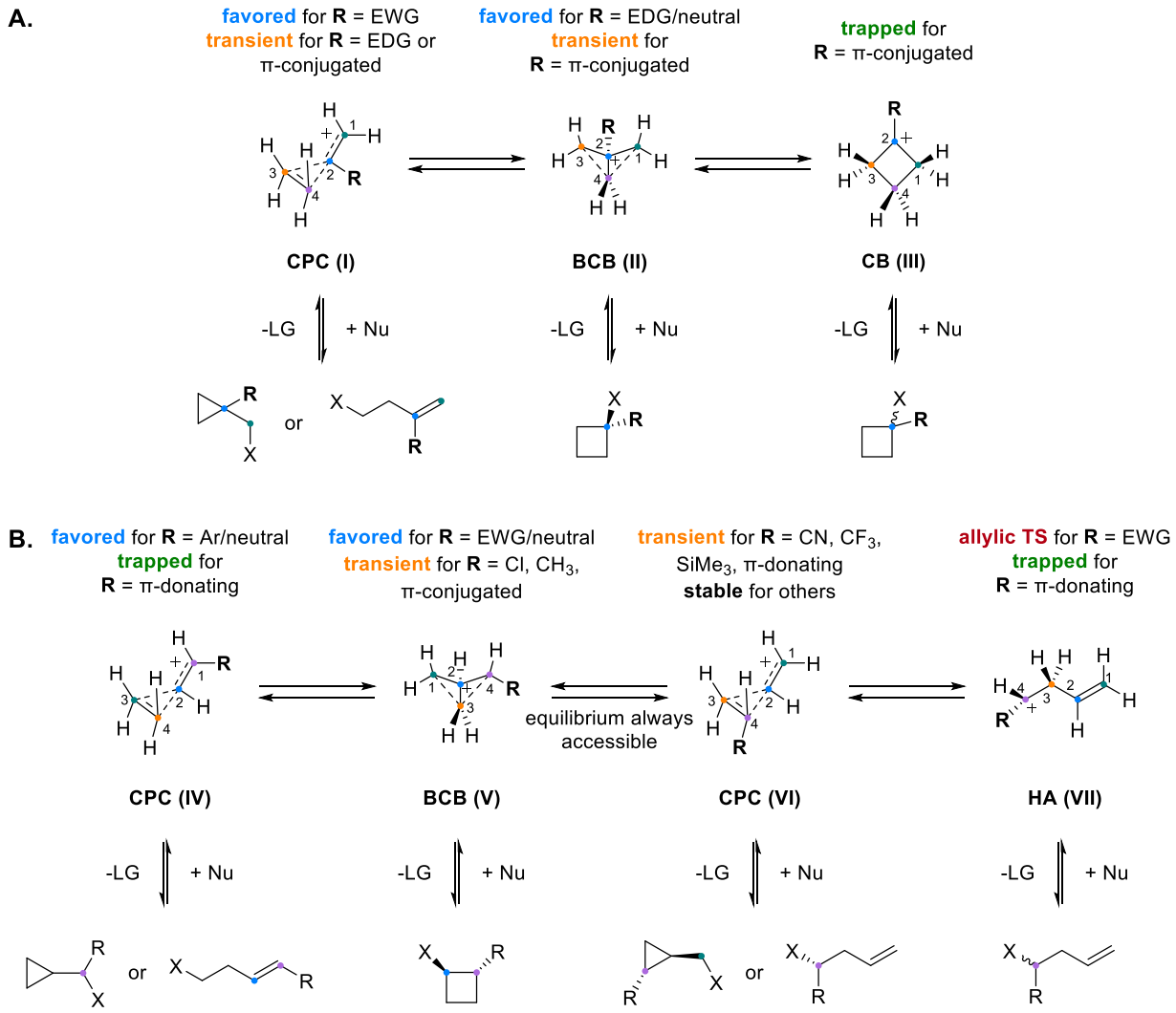

Figure 7. Predicted cationic structures for A) C2-substituted or B) C1/C3/C4-substituted $C_4H_7^+$ cations. Structures labeled as transient are either TSs or not stationary points on their PESs.

ASSOCIATED CONTENT

Supporting Information. Computational details, additional data and discussion, energies and XYZ coordinates of all computed structures. This material is available free of charge via the Internet at http://pubs.acs.org."

AUTHOR INFORMATION

Corresponding Author

* pier.a.champagne@njit.edu

Author Contributions

The manuscript was written through contributions of all authors. SPL and PAC performed and analyzed the calculations.

ACKNOWLEDGMENT

The calculations presented here were performed on the Lochness cluster at NJIT and the support of the Advanced Research Computing team is gratefully acknowledged.

REFERENCES

1. Roberts, J. D.; Mazur, R. H., Small-Ring Compounds. IV. Interconversion Reactions of Cyclobutyl, Cyclopropylcarbinyl and Allylcarbinyl Derivatives. *J. Am. Chem. Soc.* **1951,** *73*, 2509-2520.
2. Brown, H. C., The Cyclopropylcarbinyl Cation. In *The Nonclassical Ion Problem*, Brown, H. C., Ed. Springer US: Boston, MA, 1977; pp 69-82.
3. Olah, G. A.; Reddy, V. P.; Prakash, G. K. S., Long-lived cyclopropylcarbinyl cations. *Chem. Rev.* **1992,** *92*, 69-95.
4. Siehl, H.-U., Chapter One - The Conundrum of the (C4H7)+ Cation: Bicyclobutonium and Related Carbocations. In *Adv. Phys. Org. Chem.*, Williams, I. H.; Williams, N. H., Eds. Academic Press: 2018; Vol. 52, pp 1-47.
5. Koch, W.; Liu, B.; DeFrees, D. J., The C4H7+ cation. A theoretical investigation. *J. Am. Chem. Soc.* **1988,** *110*, 7325-7328.
6. Saunders, M.; Laidig, K. E.; Wiberg, K. B.; Schleyer, P. v. R., Structures, energies, and modes of interconversion of C4H7+ ions. *J. Am. Chem. Soc.* **1988,** *110*, 7652-7659.
7. Olah, G. A.; Surya Prakash, G. K.; Rasul, G., Ab Initio/GIAO-CCSD(T) Study of Structures, Energies, and 13C NMR Chemical Shifts of C4H7+ and C5H9+ Ions: Relative

Stability and Dynamic Aspects of the Cyclopropylcarbinyl vs Bicyclobutonium Ions. *J. Am. Chem. Soc.* **2008,** *130*, 9168-9172.
8. Lillien, I.; Doughty, R. A., Nonplanar cyclobutane. Steric control in deamination of cis- and trans-3-isopropylcyclobutylamine. *Tetrahedron Lett.* **1967,** *8*, 3953-3958.
9. Lillien, I., Nonplanar cyclobutane: deamination of 3-ethoxycyclobutylamine. *Chem. Commun.* **1968**, 1009-1010.
10. Lillien, I.; Doughty, R. A., Nonplanar cyclobutane. Evidence for a conformationally controlled, classic mechanism in the deamination of cis- and trans-3-isopropylcyclobutylamine. *J. Org. Chem.* **1968,** *33*, 3841-3848.
11. Lillien, I.; Reynolds, G. F.; Handloser, L., Nonplanar cyclobutane. Solvolysis of cis- and trans-3-isopropylcyclobutyl brosylate. *Tetrahedron Lett.* **1968,** *9*, 3475-3480.
12. Hanack, M.; Meyer, H., Untersuchungen an Cyclopropanverbindungen, XIV1) Umlagerungen von Trifluormethyl-substit. Cyclopropylcarbinyl-und Cyclobutyl-Verbindungen. *Justus Liebigs Annalen der Chemie* **1968,** *720*, 81-97.
13. Poulter, C. D.; Winstein, S., Solvolysis and degenerate cyclopropylcarbinyl-cyclopropylcarbinyl rearrangement of a hexamethylcyclopropylcarbinyl system. *J. Am. Chem. Soc.* **1969,** *91*, 3650-3652.
14. Lillien, I.; Handloser, L., Nonplanar cyclobutane. Steric product control in the deamination of cis- and trans-3-methylcyclobutylamine. *J. Org. Chem.* **1969,** *34*, 3058-3061.
15. Schleyer, P. v. R.; LePerchec, P.; Raber, D. J., Solvolysis of t-butyl substituted cyclobutyl tosylates. *Tetrahedron Lett.* **1969,** *10*, 4389-4392.
16. Pardo, C.; Charpentier-Morize, M., Reactivity of an α-acyl-α-cyclopropyl-carbenium ion: a highly stereoselective cyclopropylmethyl‑cyclopropylmethyl rearrangement. *J. Chem. Soc., Chem. Commun.* **1982**, 1037-1039.
17. Hittich, R.; Griesbaum, K., Rearrangement reactions of 1,2-dimethyl- and 1,3-dimethyl-1-cyclobutyl cations. *Tetrahedron Lett.* **1983,** *24*, 1147-1148.
18. Wiberg, K. B.; Shobe, D.; Nelson, G. L., Substituent effects on cyclobutyl and cyclopropylcarbinyl cations. *J. Am. Chem. Soc.* **1993,** *115*, 10645-10652.
19. Creary, X.; Heffron, A.; Going, G.; Prado, M., γ-Trimethylsilylcyclobutyl Carbocation Stabilization. *J. Org. Chem.* **2015,** *80*, 1781-1788.
20. Creary, X., 3-t-Butyl-1-methylcyclobutyl Cation. Experimental vs Computational Insights into Tertiary Bicyclobutonium Cations. *J. Org. Chem.* **2020,** *85*, 7086-7096.
21. Yang, Y.; Huang, X., Iodohydroxylation of Alkylidenecyclopropanes. An Efficient Synthesis of Iodocyclopropylmethanol and 3-Iodobut-3-en-1-ol Derivatives. *J. Org. Chem.* **2008,** *73*, 4702-4704.
22. Yang, Y.; Su, C.; Huang, X.; Liu, Q., Halohydroxylation of alkylidenecyclopropanes using N-halosuccinimide (NXS) as the halogen source: an efficient synthesis of halocyclopropylmethanol and 3-halobut-3-en-1-ol derivatives. *Tetrahedron Lett.* **2009,** *50*, 5754-5756.
23. Bauer, A.; Di Mauro, G.; Li, J.; Maulide, N., An α-Cyclopropanation of Carbonyl Derivatives by Oxidative Umpolung. *Angew. Chem. Int. Ed.* **2020,** *59*, 18208-18212.
24. Wu, J.-B.; Li, S.; Han, S.; Wang, Y.; Zhang, W.; Wang, Z.; Zeng, Y.-F., Fluorination of alkylidenecyclopropanes and alkylidenecyclobutanes: divergent synthesis of fluorinated cyclopropanes and cyclobutanes. *Org. Biomol. Chem.* **2023,** *21*, 5356-5360.
25. Long, P.-W.; He, T.; Oestreich, M., B(C6F5)3-Catalyzed Hydrosilylation of Vinylcyclopropanes. *Org. Lett.* **2020,** *22*, 7383-7386.
26. Lin, P.-P.; Huang, L.-L.; Feng, S.-X.; Yang, S.; Wang, H.; Huang, Z.-S.; Li, Q., gem-Difluorination of Methylenecyclopropanes (MCPs) Featuring a Wagner‑Meerwein Rearrangement: Synthesis of 2-Arylsubstituted gem-Difluorocyclobutanes. *Org. Lett.* **2021,** *23*, 3088-3093.
27. Blackburn, M. A. S.; Wagen, C. C.; Bodrogean, M. R.; Tadross, P. M.; Bendelsmith, A. J.; Kutateladze, D. A.; Jacobsen, E. N., Dual-Hydrogen-Bond Donor and Brønsted Acid Cocatalysis Enables Highly Enantioselective Protio-Semipinacol Rearrangement Reactions. *J. Am. Chem. Soc.* **2023,** *145*, 15036-15042.
28. Fu, W.; Zou, G.; Zhu, M.; Hong, D.; Deng, D.; Xun, C.; Ji, B., Stereoselective fluorination of methylenecyclopropanes with N-F reagents: A modular entry to γ-fluorohomoallylic sulfonimides and γ-fluorohomoallylic amides. *J. Fluorine Chem.* **2009,** *130*, 996-1000.
29. Jiang, M.; Shi, M., Reactions of methylenecyclopropanes and vinylidenecyclopropanes with N-fluorodibenzenesulfonimide. *Tetrahedron* **2009,** *65*, 5222-5227.
30. Gutta, P.; Tantillo, D. J., Theoretical Studies on Farnesyl Cation Cyclization: Pathways to Pentalenene. *J. Am. Chem. Soc.* **2006,** *128*, 6172-6179.
31. Hong, Y. J.; Tantillo, D. J., Modes of inactivation of trichodiene synthase by a cyclopropane-containing farnesyldiphosphate analog. *Org. Biomol. Chem.* **2009,** *7*, 4101-4109.
32. Hong, Y. J.; Tantillo, D. J., How Many Secondary Carbocations Are Involved in the Biosynthesis of Avermitilol? *Org. Lett.* **2011,** *13*, 1294-1297.
33. Hong, Y. J.; Tantillo, D. J., Branching Out from the Bisabolyl Cation. Unifying Mechanistic Pathways to Barbatene, Bazzanene, Chamigrene, Chamipinene, Cumacrene, Cuprenene, Dunniene, Isobazzanene, Iso-γ-bisabolene, Isochamigrene, Laurene, Microbiotene, Sesquithujene, Sesquisabinene, Thujopsene, Trichodiene, and Widdradiene Sesquiterpenes. *J. Am. Chem. Soc.* **2014,** *136*, 2450-2463.
34. Isegawa, M.; Maeda, S.; Tantillo, D. J.; Morokuma, K., Predicting pathways for terpene formation from first principles ‑ routes to known and new sesquiterpenes. *Chem. Sci.* **2014,** *5*, 1555-1560.
35. Hong, Y. J.; Giner, J.-L.; Tantillo, D. J., Bicyclobutonium Ions in Biosynthesis ‑ Interconversion of Cyclopropyl-Containing Sterols from Orchids. *J. Am. Chem. Soc.* **2015,** *137*, 2085-2088.
36. Hong, Y. J.; Tantillo, D. J., The energetic viability of an unexpected skeletal rearrangement in cyclooctatin biosynthesis. *Org. Biomol. Chem.* **2015,** *13*, 10273-10278.
37. Sato, H.; Hashishin, T.; Kanazawa, J.; Miyamoto, K.; Uchiyama, M., DFT Study of a Missing Piece in Brasilane-Type Structure Biosynthesis: An Unusual Skeletal Rearrangement. *J. Am. Chem. Soc.* **2020,** *142*, 19830-19834.
38. Sato, H.; Li, B.-X.; Takagi, T.; Wang, C.; Miyamoto, K.; Uchiyama, M., DFT Study on the Biosynthesis of Verrucosane Diterpenoids and Mangicol Sesterterpenoids: Involvement of Secondary-Carbocation-Free Reaction Cascades. *JACS Au* **2021,** *1*, 1231-1239.
39. Liang, J.; Merrill, A. T.; Laconsay, C. J.; Hou, A.; Pu, Q.; Dickschat, J. S.; Tantillo, D. J.; Wang, Q.; Peters, R. J., Deceptive Complexity in Formation of Cleistantha-8,12-diene. *Org. Lett.* **2022,** *24*, 2646-2649.

40. Sakamoto, K.; Sato, H.; Uchiyama, M., DFT Study on the Biosynthesis of Asperterpenol and Preasperterpenoid Sesterterpenoids: Exclusion of Secondary Carbocation Intermediates and Origin of Structural Diversification. *J. Org. Chem.* **2022,** *87*, 6432-6437.
41. Taizoumbe, K. A.; Steiner, S. T.; Dickschat, J. S., Mechanistic Characterisation of Collinodiene Synthase, a Diterpene Synthase from Streptomyces collinus. *Chemistry – A European Journal* **2023,** *29*, e202302469.
42. Xu, H.; Goldfuss, B.; Dickschat, J. S., Biosynthesis of the Sesquiterpene Kitaviridene through Skeletal Rearrangement with Formation of a Methyl Group Equivalent. *Organic Letters* **2023,** *25*, 3330-3334.
43. Xu, H.; Schnakenburg, G.; Goldfuss, B.; Dickschat, J. S., Mechanistic Characterisation of the Bacterial Sesterviridene Synthase from Kitasatospora viridis. *Angewandte Chemie International Edition* **2023,** *62*, e202306429.
44. Goh, S. S.; Champagne, P. A.; Guduguntla, S.; Kikuchi, T.; Fujita, M.; Houk, K. N.; Feringa, B. L., Stereospecific ring contraction of bromocycloheptenes through dyotropic rearrangements via nonclassical carbocation-anion pairs. *Journal of the American Chemical Society* **2018,** *140*, 4986-4990.
45. Lanke, V.; Marek, I., Nucleophilic Substitution at Quaternary Carbon Stereocenters. *J. Am. Chem. Soc.* **2020,** *142*, 5543-5548.
46. Chen, X.; Marek, I., Stereoinvertive Nucleophilic Substitution at Quaternary Carbon Stereocenters of Cyclopropyl Ketones and Ethers. *Angew. Chem. Int. Ed.* **2022,** *61*, e202203673.
47. Patel, K.; Lanke, V.; Marek, I., Stereospecific Construction of Quaternary Carbon Stereocenters from Quaternary Carbon Stereocenters. *J. Am. Chem. Soc.* **2022,** *144*, 7066-7071.
48. Chen, X.; Marek, I., Highly Diastereoselective Preparation of Tertiary Alkyl Isonitriles by Stereoinvertive Nucleophilic Substitution at a Nonclassical Carbocation. *Org. Lett.* **2023,** *25*, 2285-2288.
49. Chen, X.; Patel, K.; Marek, I., Stereoselective Construction of Tertiary Homoallyl Alcohols and Ethers by Nucleophilic Substitution at Quaternary Carbon Stereocenters. *Angew. Chem. Int. Ed.* **2023,** *62*, e202212425.
50. Patel, K.; Oginetz, L.; Marek, I., Highly Diastereoselective Preparation of Tertiary Alkyl Thiocyanates en Route to Thiols by Stereoinvertive Nucleophilic Substitution at Nonclassical Carbocations. *Org. Lett.* **2023**.
51. Larmore, S. P.; Champagne, P. A., Cyclopropylcarbinyl-to-Homoallyl Carbocation Equilibria Influence the Stereospecificity in the Nucleophilic Substitution of Cyclopropylcarbinols. *Journal of Organic Chemistry* **2023,** *88*, 6947-6954.
52. McNamee, R.; Frank, N.; Christensen, K.; Duarte, F.; Anderson, E. ChemRxiv 2023. https://doi.org/10.26434/chemrxiv-2023-zgdq8
53. Wiberg, K. B.; Szeimies, G., Acid-catalyzed solvolyses of bicyclobutane derivatives. Stereochemistry of the cyclopropylcarbinyl-cyclopropylcarbinyl and related rearrangements. *J. Am. Chem. Soc.* **1970,** *92*, 571-579.
54. Hoz, S.; Livneh, M.; Cohen, D., Cyclobutane-bicyclobutane system. 11. Mechanism and stereochemistry of general acid-catalyzed additions to bicyclobutane. *J. Org. Chem.* **1986,** *51*, 4537-4544.
55. Tang, L.; Huang, Q.-N.; Wu, F.; Xiao, Y.; Zhou, J.-L.; Xu, T.-T.; Wu, W.-B.; Qu, S.; Feng, J.-J., C(sp2)–H cyclobutylation of hydroxyarenes enabled by silver-π-acid catalysis: diastereocontrolled synthesis of 1,3-difunctionalized cyclobutanes. *Chem. Sci.* **2023,** *14*, 9696-9703.
56. Lin, S.-L.; Chen, Y.-H.; Liu, H.-H.; Xiang, S.-H.; Tan, B., Enantioselective Synthesis of Chiral Cyclobutenes Enabled by Brønsted Acid-Catalyzed Isomerization of BCBs. *J. Am. Chem. Soc.* **2023,** *145*, 21152-21158.
57. McNamee, R. E.; Haugland, M. M.; Nugent, J.; Chan, R.; Christensen, K. E.; Anderson, E. A., Synthesis of 1,3-disubstituted bicyclo[1.1.0]butanes via directed bridgehead functionalization. *Chem. Sci.* **2021,** *12*, 7480-7485.
58. McNamee, R. E.; Thompson, A. L.; Anderson, E. A., Synthesis and Applications of Polysubstituted Bicyclo[1.1.0]butanes. *J. Am. Chem. Soc.* **2021,** *143*, 21246-21251.
59. Siehl, H.-U.; Fuss, M.; Gauss, J., The 1-(Trimethylsilyl)bicyclobutonium Ion: NMR Spectroscopy, Isotope Effects, and Quantum Chemical Ab Initio Calculations of a New Hypercoordinated Carbocation. *J. Am. Chem. Soc.* **1995,** *117*, 5983-5991.
60. Creary, X., The cyclopropylcarbinyl route to γ-silyl carbocations. *Beilstein Journal of Organic Chemistry* **2019,** *15*, 1769-1780.
61. Poulter, C. D.; Winstein, S., Cyclopropylcarbinyl-allyl rearrangement of a hexamethylcyclopropylcarbinyl system. *J. Am. Chem. Soc.* **1969,** *91*, 3649-3650.
62. Sorensen, T. S.; Ranganayakulu, K., Cyclopropylcarbinyl-allylcarbinyl-allyl cation rearrangements. *Tetrahedron Lett.* **1970,** *11*, 659-662.
63. Hansch, C.; Leo, A.; Taft, R. W., A survey of Hammett substituent constants and resonance and field parameters. *Chem. Rev.* **1991,** *91*, 165-195.
64. Creary, X., 3-Substituted-1-(Trimethylsilylmethyl)cyclobutyl Cations: Stereochemistry of Solvent Capture of β-Trimethylsilyl Carbocations. *J. Org. Chem.* **2023,** *88*, 2079-2088.